

Reaction $^{12}\text{C}(^{16}\text{O}, ^{20}\text{Ne}_{g.s.})^8\text{Be}_{g.s.}$ in the region $10 \text{ MeV} \leq E_{c.m.} \leq 15.5 \text{ MeV}$

D. A. Viggars,* T. W. Conlon, F. P. Brady,[†] and I. Naqib[‡]

Nuclear Physics Division, AERE, Harwell, OXON OX11 0RA, United Kingdom

(Received 20 April 1978)

For the reaction $^{12}\text{C}(^{16}\text{O}, ^{20}\text{Ne}_{g.s.})^8\text{Be}_{g.s.}$ angular distributions have been measured at $E_{c.m.} = 12.22, 12.57, 12.92, 13.17, 13.37, 13.77, 14.02, 14.23, 14.67,$ and 15.07 MeV . The cross sections in the range $12.5 \leq E_{c.m.} \leq 13.5 \text{ MeV}$ are much larger than the predictions of direct α -transfer and/or statistical compound nucleus calculations. Resonance behavior at 13.2 MeV with width 650 keV is indicated. Interference effects between direct and one and two resonance amplitudes have been considered with the second resonance at 13.7 MeV being a well-known anomaly. $J = 8$ is indicated for these two resonances.

NUCLEAR REACTIONS $^{12}\text{C}(^{16}\text{O}, ^{20}\text{Ne})^8\text{Be}$, $E_{c.m.} = 10\text{--}15 \text{ MeV}$, measured $\sigma(\theta)$; compared yield to DWBA and statistical model calculations; resonance phenomena at 13.15 MeV , 13.77 MeV , deduced spin-values.

I. INTRODUCTION

The reaction $^{12}\text{C} + ^{16}\text{O}$ at energies below the Coulomb barrier has been studied traditionally because of its importance during the equilibrium stages of stellar evolution. The narrow resonances that were observed in the total cross section have been interpreted in a variety of ways. One model considers molecular type states in the optical potential.^{1,2} This has been extended to allow for excitation of one of the nuclei.^{3,4} The possibility of α -particle doorway states in the compound nucleus ^{28}Si has also been considered.^{5,6}

At higher energies there is convincing evidence for narrow resonances at $\sim 13.7 \text{ MeV}$ ($J = 8$ or 9), $\sim 19.7 \text{ MeV}$ ($J^\pi = 12, 14^+$) and weaker evidence for resonances at various energies between 14.7 and 23.8 MeV .⁷⁻¹³ Such evidence is gleaned mainly from studies of elastic^{12,14} and inelastic scattering^{12,13,15} and from the $^{12}\text{C}(^{16}\text{O}, \alpha)^{24}\text{Mg}$ channel.^{7,8,12,15} Structure has also been observed in the complete fusion cross section σ_F^{16-18} , and further evidence for resonances has been reported in measurements of the total reaction cross section.¹⁰ Explanations similar to those proposed for the low energy resonances have been proposed,¹⁹ and in addition, three-body $^{12}\text{C} - \alpha - ^{12}\text{C}$ molecular states have been considered.²⁰ Baye²¹ and Baye and Heenan²² have recently made microscopic calculations on the ^{12}C and ^{16}O system using a two center shell model and have applied the results to elastic scattering.

In some cases the angular momentum associated with a particular resonance corresponds to the semiclassical value of the angular momentum of the grazing orbit at the resonant energy. If "anomalous" resonant states are formed from grazing orbits, further information on the nature and properties of these states can be expected

from a study of reactions which may have a significant direct transfer component, and especially those in which the grazing orbit is hardly perturbed and there is no angular momentum transfer. This implies that the distances of closest approach of the ions before and after transfer be similar, or that the optimum Q value be similar to the reaction Q value. These conditions are satisfied for the reaction $^{12}\text{C}(^{16}\text{O}, ^{20}\text{Ne}_{g.s.})^8\text{Be}_{g.s.}$ in the region close to $E_{c.m.} = 15 \text{ MeV}$. There is apparently no information on this reaction channel in the energy region of interest, although recently James *et al.*²³ have reported on resonant structure observed in this reaction at higher energies close to 20 MeV .

If the anomalous states have a simple molecular type structure, then the reaction $^{12}\text{C}(^{16}\text{O}, ^{20}\text{Ne})^8\text{Be}$ going to the (spin zero) ground states should selectively populate the resonances with spin close to the grazing angular momentum. The results should, therefore, be clearer than in cases where, because of nonzero spin in the final state, many more states could be populated.

In earlier works^{24,25} we described measurements of excitation functions and several angular distributions for this reaction. In one case²⁴ the angular distributions fitted fairly well with a rather simple diffraction model. Further measurements and analyses²⁵ revealed that the situation appeared to be more complicated and a two-level model of interfering $J = 8$ resonances seemed to be the most plausible description of the behavior of the cross sections.

The present work describes additional measurements of $^{20}\text{Ne}_{g.s.} + ^8\text{Be}$ angular distributions at selected energies in the region $10 \text{ MeV} \leq E_{c.m.} \leq 15.5 \text{ MeV}$ and repeats check runs of earlier data to obtain better absolute normalizations. Statistical compound nucleus and distorted-

wave Born approximation DWBA calculations are compared to all available data. A comparison of the simple diffraction and DWBA-plus-resonance model is made. The behavior of the cross section between ≈ 12.6 and ≈ 14.0 MeV is best described in terms of DWBA plus coherent two-level ($J=8$) resonance amplitudes, rather than in terms of statistical model resonances or fluctuations, or in terms of the diffraction model used earlier.²⁴ The well-known structure at $E_{c.m.} = 13.7$ MeV may have $J=8$ rather than the previously proposed $J=9$.²⁴

The results are also of interest for their possible significance in calculations of explosive nucleosynthesis. Energies at least as high as $E_{c.m.} \sim 11$ MeV are relevant to these calculations.²⁶ In the past the channel discussed here has been neglected. This neglect may well be unjustified.

II. EXPERIMENTAL METHOD

An ^{16}O beam from the Harwell Tandem accelerator was used to bombard self-supporting ^{12}C foils of nominal thickness $10 \mu\text{g}/\text{cm}^2$ or $20 \mu\text{g}/\text{cm}^2$ which are equivalent to a beam energy spread of 30 keV (c.m.) and 60 keV (c.m.), respectively. The reaction products were observed using a Buechner magnetic spectrograph linked on a sliding-window seal to a small scattering chamber. See Ref. 27 for more details of the spectrometer.

The energy (E) and position (P) signals from the position sensitive detectors in the focal plane of the spectrometer were processed by Harwell 2000 series electronics, digitized and recorded on magnetic tape in an event-by-event mode. The two signals were used to produce a mass identifi-

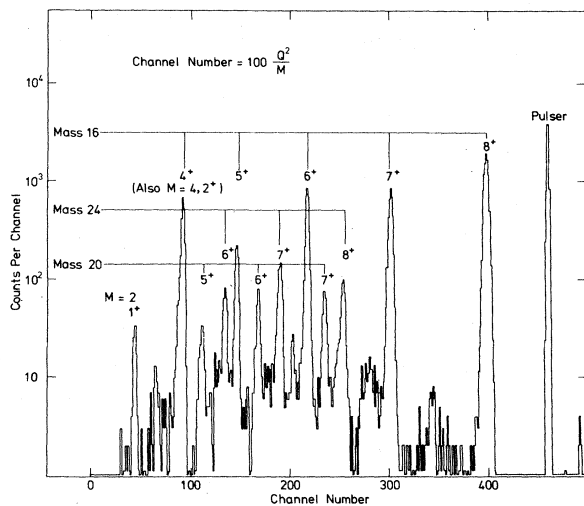


FIG. 1. Particle spectrum of $100 Q^2/M$ for $^{16}\text{O} + ^{12}\text{C}$ at 10.7 MeV (c.m.), 22° (lab) corresponding to one of the eight positions of the position sensitive detectors.

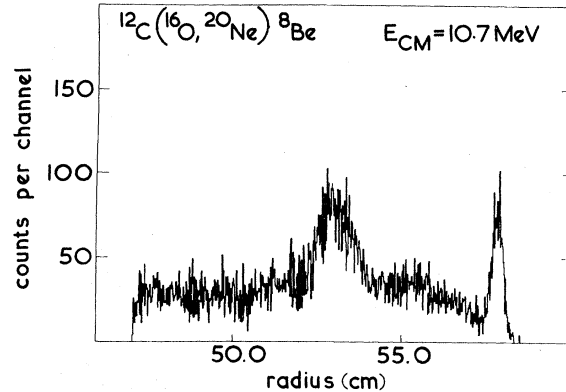


FIG. 2. Radius (i.e., momentum) spectrum for ^{20}Ne , 7^+ ions corresponding to Fig. 1 data from all eight positions of the position sensitive detectors are included.

cation spectrum via $Q^2/M = 2E/(BR)^2$, where Q = charge state and M = mass. Because of charge fractionation, several peaks are observed for a given M .

Figure 1 shows a spectrum, $100 Q^2/M$, for the $^{16}\text{O} + ^{12}\text{C}$ reaction at 10.1 MeV (c.m.) and 22° (lab). All of the major peaks are identified as various charge states of masses 16, 20, and 24, corresponding to ^{16}O elastic and inelastic scattering, mass 20 from the ^{20}Ne channels and mass 24 from the reaction $^{12}\text{C}(^{16}\text{O}, ^{24}\text{Mg})\alpha$. Figure 2 shows a momentum spectrum resulting from the analysis of the ^{20}Ne , 7^+ charge for all eight positions of the P counters. The peaks correspond to the two-body reaction $^{20}\text{Ne} + ^8\text{Be}_{g.s.}$ populating ^{20}Ne in its ground state and first excited state. The continuum arises from the three-body channel $^{16}\text{O} + ^{12}\text{C} \rightarrow ^{20}\text{Ne} + \alpha + \alpha$ and the two step process $^{16}\text{O} + ^{12}\text{C} \rightarrow ^{24}\text{Mg}^* + \alpha \rightarrow ^{20}\text{Ne} + \alpha + \alpha$. In the present work we report exclusively on the excitation functions and angular distributions corresponding to the two-body reaction leaving ^{20}Ne in its ground state.

The energy resolution achieved in the present experiment was limited by kinematic effects due to the finite acceptance angle of the spectrometer in the reaction plane. At 22° lab and a bombarding energy of 15 MeV c.m. the acceptance angle of 0.2° corresponds to $\Delta E \sim 200$ keV which is the principal contribution to the width of the $^{20}\text{Ne}_{g.s.}$ peak in Fig. 2. Angular distributions at a number of energies, as detailed below, were taken at 1° or 2° intervals between 12° and 28° lab, the latter being close to the maximum angle of emission of the $^{20}\text{Ne}_{g.s.}$ group.

The beam charge was monitored in a magnetically suppressed Faraday cup. Relative normalization between angles was achieved by simultaneously recording an energy spectrum in a surface barrier counter placed at a fixed angle in the

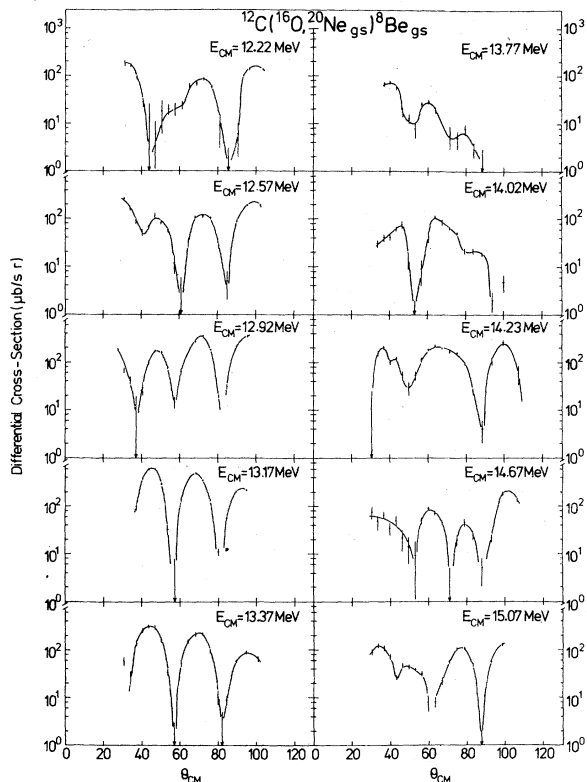


FIG. 3. Angular distributions for the reaction $^{12}\text{C}(^{16}\text{O}, ^{20}\text{Ne}_{g.s.})^8\text{Be}_{g.s.}$. The solid lines are guides for the eye. There is a normalization uncertainty of $\pm 20\%$.

scattering chamber. Absolute cross sections were obtained by comparing the reaction yield to measurements of the elastic yield at forward angles where the cross section approached the Rutherford value. The accuracy achieved by this method is about 20%.

The target thickness as measured by the fixed counter was observed to increase as a function of time. This effect was minimized by the use of a N_2 filled cold trap mounted in the chamber upstream of the target.

The yield of $^{20}\text{Ne}_{g.s.}$ was corrected on a point by point basis for the variation in the 7^+ charge state fraction using published data.²⁸

III. EXPERIMENTAL RESULTS

Angular distributions for the reaction $^{12}\text{C}(^{16}\text{O}, ^{20}\text{Ne}_{g.s.})^8\text{Be}_{g.s.}$ are shown in Fig. 3. The new measurements of these have been averaged with the four²⁵ given previously.

The narrow deep minimum seen in the 12° (lab) excitation function of earlier work²⁴ at 12.92 MeV (c.m.) can now be understood in terms of the 12.92 MeV angular distribution which shows a strong diffraction pattern with a minimum at the corresponding c.m. angle ($\approx 37^\circ$). This deep min-

TABLE I. Optical model parameters used in fitting angular distributions. Coulomb radius, $r_0 = 1.3$ fm.

	Real part	Imaginary part	Bound state
V (MeV)	-15	-5	
r_0 (fm)	1.3	1.2	1.28
a (fm)	0.55	0.55	0.55

imum and the other minima at 12.92 MeV and those in the angular distributions at 13.17 and 13.37 MeV are close to the zeros of the $L = 8$ Legendre function.

The deep sharp minima observed at 13.7 MeV in the excitation functions measured previously²⁴ are manifested in the angular distribution as a reduced cross section at most angles and a reduced total cross section (by about an order of magnitude) as compared to the total cross sections at 12.92, 13.17, and 13.37 MeV. The minimum noted earlier²⁴ at 14.7 MeV in the excitation functions is in one case (22° lab) an angular distribution minimum. The latter distribution (Fig. 3) appears to be dominated by $L = 9$.

An attempt was made to perform a partial wave analysis of the angular distributions by fitting to the general formula

$$\frac{d\sigma}{d\Omega} = \left| \sum_l \rho_l e^{i\alpha_l} P_l(\cos \theta) \right|^2.$$

However, even when the number of partial waves was restricted, unique fits could not be obtained. Qualitatively, the positions of the minima suggest that the angular distributions between 12.57 and 13.37 MeV are dominated by P_8 . This is borne out by more detailed analysis discussed later. The only other angular distribution whose minima are close to those of a Legendre polynomial is at

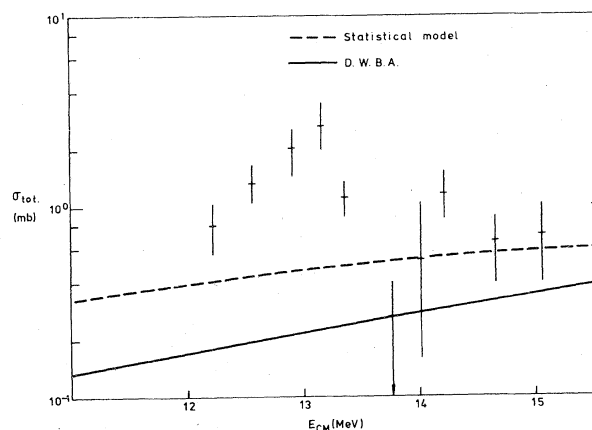


FIG. 4. Estimate of total cross section for the reaction $^{12}\text{C}(^{16}\text{O}, ^{20}\text{Ne}_{g.s.})^8\text{Be}_{g.s.}$ obtained as described in the text. The solid and dashed curves show DWBA and statistical model predictions as described in the text.

14.67 MeV. This has minima at 55° , 71° , and 89° which agree with the zeros of P_9 at 52° , 71° , and 90° .

IV. DISCUSSION

A. DWBA calculations

The recoil corrected DWBA code, LOLA,²⁹ was used to estimate the contribution of an α -transfer process to the observed cross section in the channel $^{16}\text{O} + ^{12}\text{C} \rightarrow ^{20}\text{Ne}_{g.s.} + ^8\text{Be}_{g.s.}$. The parameters of the calculation (Table I) were taken from Siemssen¹⁴ and Malmin³⁰ and considerable variations of optical parameters and bound state radii were tried. Theoretical work by Rotter³¹ suggests a spectroscopic factor of 0.16. Using this, it was not possible to fit the shape or absolute magnitude of the cross section except at 13.7 MeV. Away from this energy a spectroscopic factor several times the theoretical estimate would be required to reproduce the absolute size of the cross sections.³⁰ No combination of parameters was found which produced the type of angular distribution observed at 12.57 and 12.92 MeV where the envelope of the oscillations rises towards 90° .

Figure 4 shows the total cross section for the reaction $^{12}\text{C}(^{16}\text{O}, ^{20}\text{Ne}_{g.s.})^{8}\text{Be}_{g.s.}$. The experimental points were obtained from a Legendre polynomial fit to the angular distributions. These fits imply an extrapolation to backward angles. If the cross section falls off rapidly beyond the measured points then the fits will overestimate the true cross section. Figure 4 also shows the DWBA total cross section [with a spectroscopic factor of 0.16 (Ref. 31)] and the Hauser-Feshbach total

compound nucleus cross section. Unless the fits seriously overestimate the cross section or the theoretical spectroscopic factor is much too small, the DWBA α -transfer cross section is too small to explain the data over much of the energy range studied. It is also smaller than the predicted compound nucleus cross section. Nevertheless, the α -transfer DWBA amplitude may have an important effect on the shape of the angular distributions by interference with resonance amplitudes. This point is discussed further in Sec. IV C and Ref. 25.

B. Statistical compound nucleus calculations

Halbert *et al.*^{7,8} have shown that the reaction $^{12}\text{C}(^{16}\text{O}, \alpha)^{24}\text{Mg}$ in the energy range considered here is mainly a statistical compound nucleus process. We have calculated the contribution of this mechanism to the $^{20}\text{Ne}_{g.s.} + ^8\text{Be}_{g.s.}$ exit channel using the Hauser-Feshbach code STATIS written by Stokstad.³² In view of the success of the compound nucleus model in predicting the average measured cross sections for the reaction $^{12}\text{C}(^{16}\text{O}, \alpha)^{24}\text{Mg}$, we used this reaction as a test of our calculations against previous measurements and model predictions.

The optical model and level density parameters used in the present calculations were the same as those used by Greenwood *et al.*³³ in their calculations for the reactions $^{16}\text{O} + ^{12}\text{C} \rightarrow ^{24}\text{Mg} + \alpha$ at $E_{c.m.} \sim 13$ MeV and $^{14}\text{N} + ^{14}\text{N} \rightarrow ^{24}\text{Mg} + \alpha$ at $E_{c.m.} = 10.1$ MeV and are shown in Table II. However, the parametrization employed in STATIS (Ref. 29) differs from that used by Greenwood *et al.*³³ In STATIS the spin cutoff parameters σ^2 and the

TABLE II. Parameters of the statistical compound nucleus calculations.

	$^{12}\text{C} + ^{16}\text{O}$	$^{24}\text{Mg} + \alpha$	$^{27}\text{Si} + n$	$^{27}\text{Al} + p$	$^{26}\text{Al} + d$	$^{14}\text{N} + ^{14}\text{N}$	$^{20}\text{Ne} + ^8\text{Be}$
DEN ^a	0.14	0.149	0.137	0.137	0.152	0.163	0.163
PAIRING ^b	4.5	5.13	1.8	1.8	0	4.5	4.5
V	$7.5 + 0.4E^d$	125.3^e	48^f	47.2^g	117^h	$7.5 + 0.4E^d$	$7.5 + 0.4E^d$
R_t	6.49^d	4.47^e	3.81^f	3.75^g	3.10^h	6.5	6.36^d
a_r	0.45^d	0.54^e	0.66^f	0.65^g	0.86^h	0.45^d	0.45^d
W	$0.4 + 0.125E^d$	30.7^c	$9.6^{c,f}$	7.5^g	18.9^h	$0.4 + 0.125E^d$	$0.4 + 0.125E^d$
R_i	6.49^d	4.6^e	3.81^f	3.75^g	4.7^h	6.51^d	6.36^d
a_i	0.45^d	0.39^e	0.47^f	0.70^g	0.54^h	0.45^d	0.45^d
R_{co}	6.49^d	4.47^e	3.81^f	3.75^g	3.85^h	6.51^d	6.36^d
ρ	0	0.3	0.1	0.1	0	0	0.3

^aThe level density parameter DEN is defined by $\text{DEN} = a/M$ where M is mass of the heavy nucleus and a is the usual level density parameter, Ref. 31.

^bPairing energy.

^cDerivative Saxon-Woods well.

^dMalmin, Ref. 27.

^eSingh *et al.*, Ref. 43.

^fPerey and Buck, Ref. 44.

^gRosen, Ref. 45.

^hYule and Haerberli, Ref. 46.

Yrast cutoffs in the residual nuclei are determined by the nuclear deformation and the radius parameter r_0 via the rigid-body moment of inertia:

$$\rho_r = \frac{2}{5} M r_0^2 A^{2/3} (1 + 0.31\beta + 0.44\beta^2),$$

$$\sigma^2 = \rho_r t / h^2,$$

$$E_Y = \frac{h^2}{2\rho_r} I(I+1),$$

where t is the nuclear temperature.

In the calculations of Greenwood *et al.*³³ the Yrast cutoffs were taken from known rotational levels in the residual nuclei and σ^2 was calculated from the level density parameter a and the nuclear temperature t in accordance with the relation³¹

$$\sigma^2 = \frac{1.44 at}{\pi^2}.$$

In the present calculations the values of β were obtained from observed quadrupole moments³⁵ and r_0 was treated as a parameter. As pointed out by Stokstad³⁶ the absolute cross sections are very sensitive to the value of r_0 . If r_0 is decreased, then σ^2 is increased and the Yrast cutoff is lowered so that additional exit channels are brought into effect thus decreasing the predicted cross sections. For a suitable choice of r_0 the parametrizations employed by Greenwood *et al.*³³ and in STATIS^{32,35} give closely similar results. In the present calculations a value of $r_0 = 1.3$ fm was used throughout.

TABLE III. Comparison of present calculations (with $r_0 = 1.3$ fm) and those of Greenwood *et al.* (Ref. 33) for the reaction $^{12}\text{C}(^{16}\text{O}, \alpha)^{24}\text{Mg}$ with experimental data from Refs. 7, 8, and 33. The center-of-mass bombarding energy ranges from 12.5 to 14.5 MeV corresponding to an excitation energies in ^{28}Si from 29.2 MeV to 31.2 MeV.

E_x (MeV)	J^π	σ_{exp} (mb) Ref.	σ_{HF} (mb) This work	σ_{HF} (mb) Ref. 30
0	0^+	2.87 ± 0.34^a	2.4 ^c	2.6
1.37	2^+	6.42 ± 0.50^a	6.2 ^c	6.4
4.12	4^+	13.85 ± 0.8^a	8.7 ^c	8.8
4.23	2^+		4.4 ^c	4.7
5.22	3^+	6.21 ± 0.46^a	3.8 ^c	4.0
6.00	4^+	9.39 ± 0.28^a	7.1 ^c	7.2
6.44	0^+		0.74 ^c	0.8
5.22	3^+	7.9 ^b	3.7 ^d	5.0
6.00	4^+	9.8 ^b	7.3 ^d	8.0
6.44	0^+	1.7 ^b	0.68 ^d	0.9
7.35	2^+	3.0 ^b	2.5 ^d	2.7
8.12	6^+	14.0 ^b	10.0 ^d	11.0

^a Experimental data Refs. 7, 8; $E_{\text{c.m.}} = 12.5\text{--}14$ MeV.

^b Experimental data Ref. 32; $E_{\text{c.m.}} = 13.5\text{--}14.5$ MeV as given in Ref. 32.

^c Averaged calculations at 12.6, 13.0, 13.4, 14.0 MeV.

^d Averaged calculations at 13.4, 14.0, and 14.4 MeV.

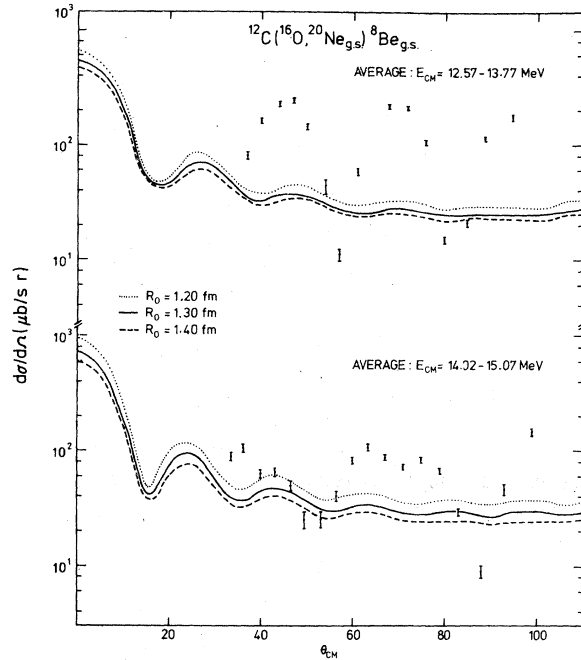


FIG. 5. Averaged angular distributions compared with statistical model calculations described in the text.

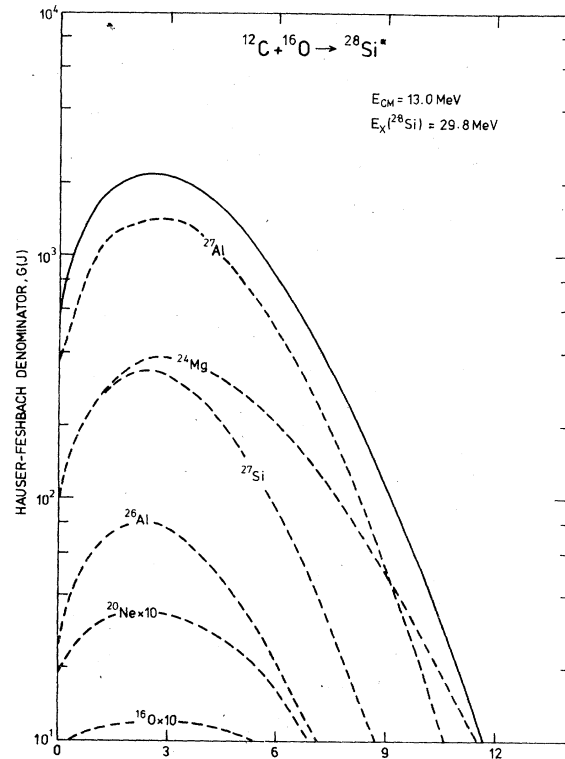


FIG. 6. Hauser-Feshbach denominator as a function of spin for a center-of-mass energy 13 MeV in the entrance channel $^{12}\text{C} + ^{16}\text{O}$.

Table III shows the results of the present calculations for $^{12}\text{C}(^{16}\text{O}, \alpha)^{24}\text{Mg}$ and compares them with previous calculations and experimental results. The present calculations are in good agreement with the data and with the previous calculations. As discussed in Viggars and Naqib³⁷ the present calculations also agree with the data³⁸ on $^{14}\text{N} + ^{14}\text{N} \rightarrow ^{24}\text{Mg} + \alpha$. Since the present calculations agree satisfactorily with experimental results for the reactions $^{16}\text{O} + ^{12}\text{C} \rightarrow ^{24}\text{Mg} + \alpha$ and $^{14}\text{N} + ^{14}\text{N} \rightarrow ^{24}\text{Mg} + \alpha$, they may reasonably be used to estimate the compound nucleus contribution to the reaction $^{16}\text{O} + ^{12}\text{C} \rightarrow ^{20}\text{Ne}_{g.s.} + ^8\text{Be}_{g.s.}$. The results are shown in Fig. 5. This figure shows averaged measured angular distributions and the corresponding Hauser-Feshbach predictions. In both cases the range of averaging, 12.9 to 13.8 MeV and 14.0 to 15.1 MeV respectively, is about eight times the coherence width found by Halbert *et al.*^{7,8} in the reaction $^{16}\text{O} + ^{12}\text{C} \rightarrow ^{24}\text{Mg} + \alpha$ at similar compound nucleus excitation energies.

It is very clear from Fig. 5 that the observed cross sections are not only an order of magnitude larger than predicted but they also differ markedly from the shape of the predicted angular distribution. It is significant that the measured angular distributions exhibit pronounced diffractionlike structure over a range of about eight times the

coherence width found by Halbert *et al.*^{7,8} Although only four angular distributions were used in producing the average in Fig. 5, the strong similarity between the angular distributions at 12.96, 13.17, and 13.37 MeV makes it most improbable that the large average cross section can be ascribed to a fortuitous combination of large fluctuations.

Although the absolute cross sections predicted by the Hauser-Feshbach calculations are sensitive to the value of r_0 , the ratio of the predicted cross sections in the $^{24}\text{Mg} + \alpha$ and $^{20}\text{Ne} + ^8\text{Be}$ channels is not. (The value of r_0 used here was 1.3 fm. The effects of using 1.2 and 1.4 fm are shown in Fig. 5.) The difference in the cross sections in these two channels can be understood as follows. The $^{24}\text{Mg} + \alpha$ channel is dominated by $J = 10$ and the $^{20}\text{Ne} + ^8\text{Be}$ channel by $J = 8$. This is because more outgoing energy is available in the $^{24}\text{Mg} + \alpha$ channel ($Q = 6.77$ MeV) than in the $^{20}\text{Ne} + ^8\text{Be}$ channel ($Q = -2.64$ MeV). The relative sizes of the calculated compound nucleus cross sections are determined mainly by the relative sizes of the Hauser-Feshbach denominator $G(J)$, i.e., the number of open channels for a given compound nucleus angular momentum. It can be seen from Fig. 6 that $G(8)/G(10) \sim 5$ leading to a larger predicted cross section in the $^{24}\text{Mg} + \alpha$ channel.

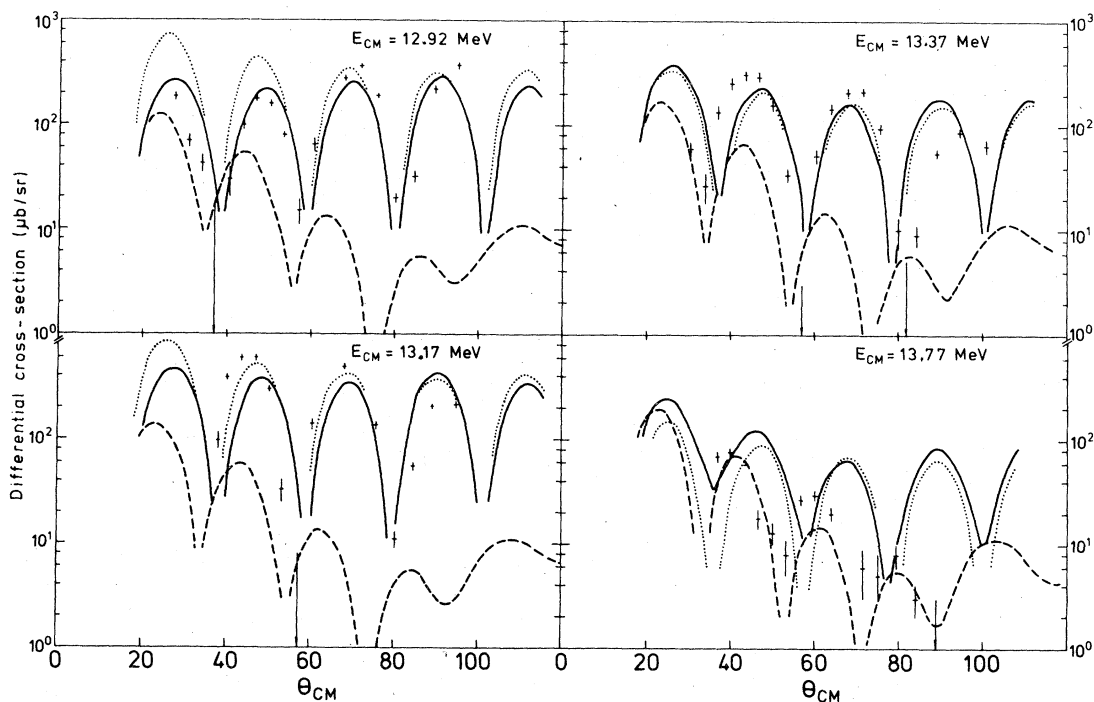


FIG. 7. Angular distributions near 13.1 MeV showing pure resonance Legendre polynomial, (P_8) (dotted lines) pure DWBA (dashed lines) and combined resonance and DWBA fits (solid lines). The parameters of the fits are given in the tables.

The calculations thus indicate that the compound nucleus mechanism does not account for most of the cross section observed in the $^{20}\text{Ne}_{g.s.} + ^8\text{Be}_{g.s.}$ channel at the energies studied.

C. Resonance phenomena

1. $E_{c.m.} 12.57 \text{ MeV} \leq E_{c.m.} \leq 13.77 \text{ MeV}$

The angular distributions at 12.57 to 13.37 MeV all show a large $P_8(\cos \theta)$ component. This energy range is much greater than the coherence width found by Halbert *et al.*^{7,8} of about 120 keV. There is a systematic change of shape over the range. At low energies the envelope of the "diffraction pattern" rises towards 90° . At higher energies it falls. Two models of the reaction in this region have been tried as given in Refs. 24 and 25. With the knowledge of additional and improved angular distribution measurements of the statistical model analysis, and of further partial wave analyses, we can make a better assessment of the two models.

Model i. As remarked earlier a decomposition of the partial wave structure of the angular distributions using simply the general formula for the scattering amplitude was not possible. However, by introducing a simple diffraction model for the S-matrix and thus reducing the number of parameters sensible fits could be made to the first angular distributions obtained.²⁴ The parameters used were the nuclear radius, a width in angular momentum space, and a nuclear contribution to the phase shift. This model produced satisfactory fits at energies near 12.9 MeV. However, at 13.77 MeV it was necessary to set the amplitude of the ninth partial wave equal to zero to fit the angular distribution. This was interpreted as an interference effect between a $J = 9$ resonance and a direct reaction background described by the diffraction model. Huby³⁹ has shown that such destructive interference is possible in the rigorous framework of R-matrix theory.

Two objections now arise to this preliminary model. Subsequently obtained angular distributions

outside the region analyzed in Ref. 24 cannot be fitted without allowing rapid changes in the parameters. Then, as described in Sec. IV A the expected DWBA contribution from a direct α -transfer background has been calculated. To support model i this calculation should reproduce the diffraction type angular distributions of the model. In fact, the shape of the angular distributions, particularly the rise towards 90° , cannot be obtained. Furthermore, the size of the calculated cross sections is much too small to agree with experiment. For instance, Fig. 7 shows the angular distribution at 12.9 MeV and the direct reaction prediction (dashed line).

Model ii. The cross section in the region between 12.5 and 13.5 MeV is much larger than either the direct reaction or statistical model predictions. The angular distributions are dominated by $P_8(\cos \theta)$. These facts suggested the presence of a broad $J = 8$ resonance at about 13 MeV.²⁵ The angular distributions show, however, as has been remarked, a systematic change over the region that is not expected from just a $J = 8$ resonance. Trying to understand this behavior we considered interference between a $J = 8$ resonance and DWBA amplitudes. This was done by calculating the α -transfer DWBA amplitudes, A_l (DWBA), and adding a Breit-Wigner resonance amplitude in the eighth partial wave, so that we obtain for the final amplitudes

$$A_l = A_l(\text{DWBA}) + \delta_{l,8} \frac{G}{E_1 - E - i\Gamma_1/2}.$$

The DWBA amplitudes were calculated as described in Sec. IV A and Ref. 22. The estimated observed angle-integrated cross sections (Sec. IV A) were used to obtain the parameters of the resonance as described in Ref. 25. Satisfactory fits were obtained with $E_1 = 13.15$ MeV and $\Gamma_1 = 650$ keV. The results are shown in Fig. 7. It can be seen there that the DWBA cross section (dashed lines) makes a small contribution to the total cross section. The important role of the DWBA amplitude is to modify the pure $P_8(\cos \theta)$ resonance angular distribution to give the systematic behavior observed. It follows that the

TABLE IV. Parameters for the two-level fits.

	E_λ (MeV)	$\Gamma_{\lambda c}$ (keV)	$\Gamma_{\lambda c}^{1/2}$ (keV ^{1/2})	$\Gamma_{\lambda c'}^{1/2}$ (keV ^{1/2})	$\Gamma_{\lambda c''}^{1/2}$ (keV ^{1/2})	$\Gamma_{\lambda c'''}^{1/2}$ (keV ^{1/2})
$\lambda = 1$	13.15	650	4.6	4.6	-1.0	1.0
$\lambda = 2$	13.75	100	1.4	1.0	1.0	6.0

Channel c is $^{16}\text{O} + ^{12}\text{C}$.
Channel c' is $^{20}\text{Ne} + ^8\text{Be}$ (ground states).
Channel c'' represents $\text{Mg} + \alpha$ channels.
Channel c''' represents other open channels.

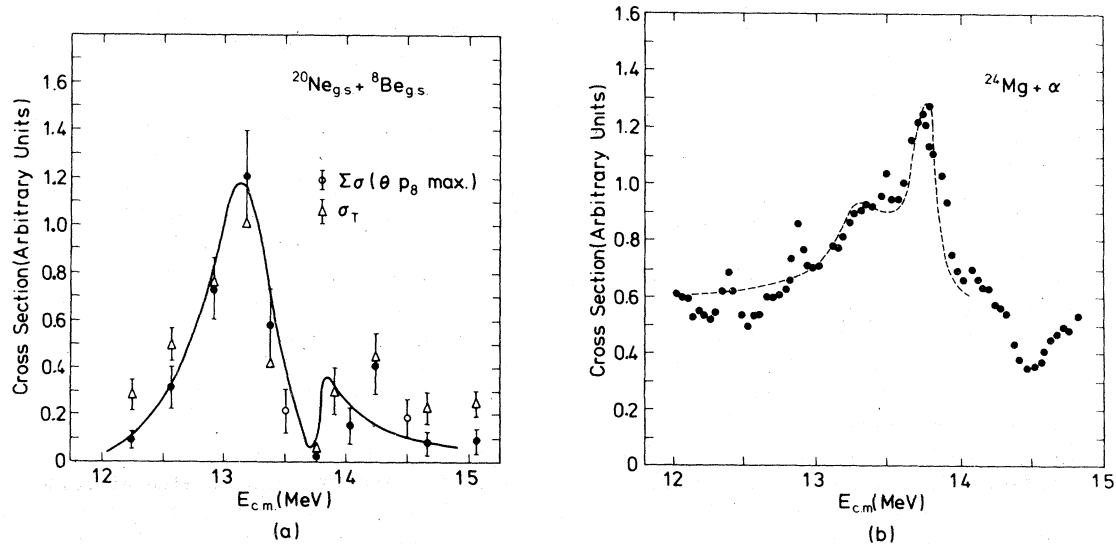


FIG. 8. Two-level formula fits to angle integrated data in the (a) $^{20}\text{Ne}_{g.s.} + ^8\text{Be}_{g.s.}$ and (b) $^{24}\text{Mg} + \alpha$ channels. For part (a), the angle integrated data were obtained in two ways: in one case (denoted σ_T) from the Legendre polynomial fits as described in Sec. IV A; in the second case the sum of cross sections measured at angles corresponding to the maximum of $P_8(\cos \theta)$ are plotted. In some cases (open circles) the cross section is based only on the 22° excitation function. For part (b), the data points are based on the original data of Halbert *et al.* (Refs. 7 and 8). Note that the ^{24}Mg data are summed over a number of final states as well as angles.

details of the DWBA calculation are not very important for the quality of the fits.

At 13.77 MeV this model breaks down. Figure 7 shows that the resonance + DWBA cross section is much larger than the observed cross section. In fact, the DWBA alone gives a reasonable fit to the data. This is interpreted as being due to destructive interference at 13.77 MeV between resonance 1 ($E_1 = 13.15$ MeV, $\Gamma_1 = 650$ keV) and a second resonance 2 ($E_2 = 13.77$ MeV, $\Gamma_2 = 60$ –100 keV) which leaves little resultant resonant amplitude at 13.77 MeV. The goodness of fit of the DWBA prediction at 13.77 MeV must be largely fortuitous since it ignores the resultant amplitude from the interference completely. It also ignores the contribution from a compound nucleus component, which should make at least as large a contribution as DWBA (see Fig. 4) to so small a cross section.

The parameters of resonance 2 were estimated by applying the two-level formula of Lane and Thomas.⁴⁰ Using the parameters of Table IV, which are listed in the notation of Ref. 40, the fit shown in Fig. 8(a) (slightly modified from Fig. 2 of Ref. 25) was obtained for the angle-integrated cross section. The two-level formula leads naturally to a consideration of other exit channels and the parameters of Table IV also allow a fit to the data of Halbert *et al.*^{7,8} in the $^{24}\text{Mg} + \alpha$ channel as shown in Fig. 8(b). (See reference 25 for details.)

In order for coherent interference of the type

described by the two-level formula to occur between resonances 1 and 2, they must have the same spin. The angular distributions give spin 8 for resonance 1 and, therefore, resonance 2 must also have spin 8 in this model.

2. $E_{c.m.} = 14.7$ MeV

The 22° and 12° excitation functions²⁴ indicate the possibility of a resonant effect at 14.7 MeV. The angular distribution at 14.67 MeV appears to be closer to a pure Legendre polynomial, $P_9(\cos \theta)$, than neighboring angular distributions. However, the difference between 14.67 MeV and the neighboring angular distributions is not as striking as at 13.77 MeV. The evidence for a resonance at this energy is therefore weak.

Other workers^{9,10} have proposed a spin 10 resonance at about 14.7 MeV. If this resonance has width in the $^{20}\text{Ne}_{g.s.} + ^8\text{Be}_{g.s.}$ channel our data suggest spin 9 rather than 10. The observed angular distribution is very different from $P_{10}(\cos \theta)$. However, there is always the possibility of interference and cancellation in a particular channel of one (i.e., $L = 10$) of the few dominant L values (i.e., $L = 9$ and 10) leaving one L (i.e., $L = 9$) as the apparent dominant angular momentum.

3. $E_{c.m.} = 12.9$ MeV

In a recent paper Taras *et al.*⁴¹ suggested that the 12.9 MeV minimum in the 12° excitation function²⁴ is connected with a narrow ($\Gamma = 130$ keV) resonance observed by them at 12.77 MeV in the

$^{27}\text{Si} + n$, $^{27}\text{Al} + p$, $^{26}\text{Al} + d$, $^{24}\text{Mg} + \alpha$, and elastic channels. As we have explained in Sec. III and Ref. 24, the 12.9 MeV minimum does not appear to be indicative of a narrow resonance. There is no evidence in our data for the 12.77 MeV resonance. Taras *et al.*⁴¹ assigned $J = 8$ to the 12.77 MeV feature on the basis of the $P_8(\cos \theta)$ angular distributions observed in our data. Since the resonance does not seem to have width in the channel observed in our experiment, the assignment must be considered uncertain.

V. CONCLUSIONS

The reaction $^{12}\text{C}(^{16}\text{O}, ^{20}\text{Ne}_{g.s.})^8\text{Be}_{g.s.}$ in the region $10 \leq E_{c.m.} \leq 15.5$ MeV has been shown to be very complicated. We have found evidence for interfering resonances outside the scope of the statistical model. The resonances in turn appear to interfere with a direct contribution. In addition, calculation shows that in regions away from strong resonances or where resonant contributions are suppressed by destructive interference, statistical compound nuclear processes are likely to make a significant (coherent) contribution to the cross section.

If we accept model ii for the 12.5–13.77 MeV region, and it appears more plausible than model i, then there is a previously unobserved resonance at 13.15 MeV with width 650 keV and $J = 8$. Furthermore, the 13.77 MeV resonance ($\Gamma \sim 60$ –100 keV) must have spin 8.

Investigation of the elastic channel near 13.7 MeV has suggested a resonance with spin 9.⁴² The question arises as to whether this resonance is to be identified with the one observed in the present work at 13.77 MeV. If so, what is the correct spin? The fact that this resonance appears as a dip in the elastic cross section at most angles again suggests consideration of destructive interference of one dominant L value amplitude, possibly leaving an adjacent L as most important.

A similar doubt arises at 14.7 MeV. Earlier workers^{9,10} have suggested a $J = 10$ resonance at this energy. The evidence for this resonance is weak in the channel studied here. But the dominant component in the angular distribution at 14.67 MeV is $P_9(\cos \theta)$.

Branford *et al.*¹⁰ have pointed out that it is unusual for a resonance to be observed in all exit

channels. It may be that the conflicts over spin assignment mentioned above are the result of this. That is to say, the resonance at 13.77 MeV in the present work may not be the same as that observed near 13.7 MeV in the elastic channel. It seems likely, however, that some effect of such a pronounced structure in the exit channel ($^{20}\text{Ne} + ^8\text{Be}$) should be observable in the entrance (elastic) channel. It is perhaps more plausible that the resonance observed at 14.7 MeV in the $^{24}\text{Mg} + \alpha$ reaction does not have significant width in the $^{20}\text{Ne}_{g.s.} + ^8\text{Be}_{g.s.}$ channel, so that the P_9 character of the angular distribution may not conflict with the assignment of $J = 10$ to the 14.7 MeV resonance.

The appearance of resonances in selected channels is probably partly due to kinematic effects such as angular momentum matching, but may also give information on the structure of the resonances. One way of approaching this problem has been attempted here by the use of the two-level formula to analyze data in the $^{20}\text{Ne}_{g.s.} + ^8\text{Be}_{g.s.}$ and $^{24}\text{Mg} + \alpha$ channels simultaneously. This gives reduced partial widths for the resonances in both channels. The values in Table IV may not be unique, but if the method is applied to more channels it should be capable of giving useful information.

Over most of the region studied the reaction yield is considerably greater than expected from a direct or compound nuclear process alone. This could have significant consequences for calculations of explosive nucleosynthesis in stars, which do not yet include the unexpected high yield, and which are sensitive to energies at least as high as $E_{c.m.} \sim 11$ MeV.²⁶

We are grateful to Dr. M. L. Halbert for making available the data used in Fig. 8(b). We thank Dr. C. F. Clement, Dr. R. Huby, Dr. A. M. Lane, and Dr. N. Rowley for helpful conversation and Mr. A. T. McIntyre and Mr. D. J. Parker for help in experimental work and data analysis. F.P.B. and I.N. gratefully acknowledge the support and hospitality of Harwell Laboratory during part of this work. F.P.B. acknowledges the support of the U. S. National Science Foundation during a subsequent period at U. C. Davis. We are grateful to the Royal Society for a grant towards this work and to Dr. D. W. Sciama for his interest and support.

*Department of Astrophysics, University of Oxford, U.K.

†Present address: Department of Physics, University

of California, Davis, Calif. 95616.

‡Present address: Department of Physics, University of Kuwait, Kuwait.

- ¹E. W. Vogt and H. McManus, Phys. Rev. Lett. 4, 518 (1960).
- ²B. N. Nagorecka and J. O. Newton, Phys. Lett. 41B, 34 (1972).
- ³B. Imanishi, Phys. Lett. 27B, 267 (1968).
- ⁴B. Imanishi, Nucl. Phys. A125, 33 (1969).
- ⁵H. Voit, G. Hartmann, H. D. Helb, G. Ischenko, and F. Siller, Z. Phys. 255, 425 (1972).
- ⁶H. Voit, G. Ischenko, and F. Siller, Phys. Rev. Lett. 30, 564 (1973).
- ⁷M. L. Halbert, F. E. Durham, and A. van der Woude, Phys. Rev. 162, 899 (1967).
- ⁸M. L. Halbert, F. E. Durham, C. D. Moak, and A. Zucker, Phys. Rev. 162, 919 (1967).
- ⁹D. Branford, J. O. Newton, J. M. Robinson and B. N. Nagorecka, J. Phys. A: Nucl. Gen. 7, 1193 (1974).
- ¹⁰D. Branford, B. N. Nagorecka, and J. O. Newton, J. Phys. G: Nucl. Phys. 3, 1565 (1977).
- ¹¹P. Charles, F. Auger, I. Badaug, B. Berthier, M. Dost, J. Gastebois, B. Fernandez, S. M. Lee, and E. Plagnol, Phys. Lett. 62B, 289 (1976).
- ¹²R. Stokstad, D. Shapira, L. Chua, P. Parker, M. W. Sachs, R. Wieland, and D. A. Bromley, Phys. Rev. Lett. 28, 1523 (1972).
- ¹³D. Shapira, R. G. Stokstad, M. W. Sachs, A. Gobbi, and D. A. Bromley, Phys. Rev. C 12, 1907 (1975).
- ¹⁴R. H. Siemssen, in *Proceedings of the Symposium on Heavy Ion Scattering, Argonne, 1971* [Argonne National Laboratory Report No. ANL 7387, 1973 (unpublished)].
- ¹⁵R. E. Malmin, R. H. Siemssen, D. A. Sink, and P. P. Singh, Phys. Rev. Lett. 28, 1590 (1972).
- ¹⁶H. Frohlich, P. Duck, W. Galster, W. Treu, H. Voit, and H. Witt, Phys. Lett. 64B, 408 (1976).
- ¹⁷J. J. Kolata, R. M. Freeman, F. Haas, B. Heusch, and A. Gallman, Phys. Lett. 65B, 333 (1976).
- ¹⁸P. Sperr, S. Vidor, Y. Eisen, W. Henning, D. G. Kovar, T. R. Ophel, and P. Zeidman, Phys. Rev. Lett. 36, 405 (1976).
- ¹⁹H. J. Fink, W. Scheid, and W. Greiner, Nucl. Phys. A188, 259 (1972).
- ²⁰H. Horiuchi, K. Ikeda, and Y. Suzuki, Prog. Theor. Phys. Suppl. 52, 89 (1972).
- ²¹D. Baye, Nucl. Phys. A272, 445 (1976).
- ²²D. Baye and P-H. Neenan, Nucl. Phys. A283, 176 (1977).
- ²³D. R. James, G. R. Morgan, N. R. Fletcher, and M. B. Greenfield, Nucl. Phys. A274, 177 (1976).
- ²⁴D. A. Viggars, T. W. Conlon, I. Naqib, and A. T. McIntyre, J. Phys. G: Nucl. Phys. 2, 55 (1976).
- ²⁵F. P. Brady, D. A. Viggars, T. W. Conlon, and D. J. Parker, Phys. Rev. Lett. 39, 870 (1977).
- ²⁶T. W. Conlon, Nature 247, 268 (1974).
- ²⁷W. R. McMurray, T. W. Conlon, B. W. Hooton, and M. Ivanovich, Nucl. Phys. A265, 517 (1976).
- ²⁸J. B. Marion and F. C. Young, *Nuclear Reaction Analysis* (North-Holland, Amsterdam, 1968).
- ²⁹R. M. DeVries, University of Rochester report, 1974 (unpublished).
- ³⁰R. E. Malmin, Ph.D. thesis, Indiana University, 1971 (unpublished).
- ³¹I. Rotter, Fortschr. Phys. 16, 195 (1968).
- ³²R. Stokstad, Wright Nuclear Structure Laboratory, Yale University, Internal Report No. 52 (unpublished).
- ³³L. R. Greenwood, K. Katorik, R. E. Malmin, T. H. Braid, J. C. Stolfus, and R. H. Siemssen, Phys. Rev. C 6, 2112 (1972).
- ³⁴U. Facchini and E. Saetta-Menichella, Energia Nucl. 15, 54 (1968).
- ³⁵A. Christy and O. Hauser, *Nucl. Data Tables* 11, 281 (1973).
- ³⁶R. Stokstad, in *Proceedings of the International Conference on Reactions between Complex Nuclei, Nashville, Tennessee, 1974*, edited by R. L. Robinson, F. K. McGowan, J. B. Ball, and J. H. Hamilton (American Elsevier, New York, 1974), Vol. II, p. 327.
- ³⁷D. A. Viggars and I. Naqib (unpublished).
- ³⁸R. Middleton, J. D. Garrett, and H. D. Fortune, Phys. Rev. C 4, 1987 (1971).
- ³⁹R. Huby, private communication.
- ⁴⁰A. M. Lane and R. G. Thomas, Rev. Mod. Phys. 30, 257 (1958).
- ⁴¹P. Taras, G. Rao, N. Schulz, J. P. Vivien, B. Haas, J. C. Merdinger, and S. Landsberger, Phys. Rev. C 15, 834 (1977).
- ⁴²R. E. Malmin and P. Paul, in *Proceedings of the Second International Conference on Clustering Phenomena in Nuclei, College Park, Maryland*, edited by D. A. Goldberg, J. B. Marion, and S. J. Wallace (University of Maryland, College Park, 1975).
- ⁴³P. P. Singh, R. E. Malmin, M. High, and D. W. Devins, Phys. Rev. Lett. 23, 1124 (1969).
- ⁴⁴F. Perey and B. Buck, Nucl. Phys. 32, 353 (1962).
- ⁴⁵L. Rosen, Helv. Phys. Acta. Exp. Suppl. 12, 253 (1966).
- ⁴⁶T. J. Yule and W. Haeberli, Nucl. Phys. 117, 1 (1968).